

Geophysical Research Letters[®]



RESEARCH LETTER

10.1029/2023GL104630

Key Points:

- Organic matter (OM) with a high cation exchange capacity can dominate the imaginary conductivity response of sediments
- Neglecting OM may bias petro-physical interpretations of spectral induced polarization measurements

Supporting Information:

Supporting Information may be found in the online version of this article.

Correspondence to:

A. Mella and C. Strobel,
adrian.mellage@uni-kassel.de;
cora.strobel@uni-tuebingen.de

Citation:

Strobel, C., Doerrich, M., Stieff, E.-H., Huisman, J. A., Cirpka, O. A., & Mella, A. (2023). Organic matter matters—The imaginary conductivity of sediments rich in solid organic carbon. *Geophysical Research Letters*, 50, e2023GL104630. <https://doi.org/10.1029/2023GL104630>

Received 19 MAY 2023

Accepted 18 NOV 2023

Author Contributions:

Conceptualization: C. Strobel, J. A. Huisman, O. A. Cirpka, A. Mella

Data curation: C. Strobel

Formal analysis: C. Strobel

Investigation: C. Strobel, M. Doerrich,

E.-H. Stieff

Methodology: C. Strobel, M. Doerrich,

E.-H. Stieff

Resources: O. A. Cirpka, A. Mella


Supervision: J. A. Huisman, O. A. Cirpka, A. Mella

Visualization: C. Strobel

Writing – original draft: C. Strobel

Writing – review & editing: J. A. Huisman, O. A. Cirpka, A. Mella

Organic Matter Matters—The Imaginary Conductivity of Sediments Rich in Solid Organic Carbon

C. Strobel^{1,2} , M. Doerrich¹, E.-H. Stieff¹, J. A. Huisman³ , O. A. Cirpka¹ , and A. Mella² 

¹Department of Geosciences, University of Tübingen, Tübingen, Germany, ²Civil and Environmental Engineering, University of Kassel, Kassel, Germany, ³Institute of Bio- and Geosciences, Forschungszentrum Jülich GmbH, Agrosphere (IBG-3), Jülich, Germany

Abstract Solid organic matter (OM) is a biogeochemically relevant constituent of soils and sediments. It also affects sediments' geophysical properties, but is often overlooked in hydro- and biogeophysical approaches for the characterization of the shallow subsurface. Here, we explore the potential of spectral induced polarization (SIP) to delineate OM-rich zones in the subsurface and provide insights into the mechanisms that drive OM-polarization using measurements on both field cores and artificial OM-sand mixtures. Both, field samples and artificial mixtures showed a linear relationship between the total organic carbon (TOC) content and charge storage (imaginary conductivity). The high cation exchange capacity of OM drives the increase in polarization and can help in delineating potentially microbially active OM-rich zones in cores or field surveys. To avoid misinterpretation of SIP data in unconsolidated media, we strongly suggest quantifying TOC content in sediment samples to accompany the interpretation of field surveys.

Plain Language Summary Soils and sediments are mixtures of minerals, water, air and partly decomposed organic matter (OM) derived from plants and soil organisms. The field of geophysics measures the electrical, seismic, and magnetic properties of soils and sediments and relates them to the minerals to derive images of their composition. The contribution of the organic fraction is largely ignored. We performed experiments that show that the organic-matter fraction can contribute significantly to the electrical signal of sediments. In fact, our data show that we can locate areas of high organic content in soils using the geophysical technique of spectral induced polarization. We performed measurement on sediment profiles from a natural aquifer and lab experiments on mixtures of peat and sand, to derive a relationship between organic content and the charge storage capacity of sediments. Our results show the potential of using geophysics to map out organic content in sediments, and caution the disregard for OM when deriving physical models of sediment using electrical measurements.

1. Introduction

Solid organic matter (OM) plays a crucial role in providing substrates for microorganisms, as well as the retardation and degradation of contaminants in natural porous media (soils and sediments). Understanding its geoelectrical properties is important for hydro- and biogeophysical surveys in OM-containing sediments, because of its ubiquitous presence and heterogeneous distribution. In particular, delineating its distribution in the subsurface may help to identify potential locations of substrate enrichment that can fuel biogeochemical turnover (Flores Orozco et al., 2020; Katona et al., 2021). A growing, yet limited number of studies have shown promising, and often conflicting, evidence that (spectral) induced polarization (SIP) is sensitive to the presence of OM (Katona et al., 2021; Mella et al., 2022; Ponziani et al., 2012; Schwartz & Furman, 2014).

Measurements of SIP are typically expressed as complex conductivity (σ^*) values (Equation 1). The real part (σ') is a function of electrical conduction in the pore fluid (i.e., electrolytic conductivity) and along particle surfaces (i.e., surface conductivity). The imaginary part (σ'') is a function of the polarization of charged surfaces, that is, the charge storage capacity of the sediment (Binley & Slater, 2020; Slater & Glaser, 2003 and references therein).

$$\sigma^* = \sigma' + i \cdot \sigma'' \quad (1)$$

Electrochemical polarization of the electrical double layer (EDL) that surrounds charged surfaces is expected to be the dominating polarization mechanism in unconsolidated sediments (Bücker et al., 2019). However, the polarization mechanisms of OM remain largely unknown (Katona et al., 2021; Mella et al., 2022; Schwartz &

© 2023. The Authors.

This is an open access article under the terms of the [Creative Commons Attribution License](https://creativecommons.org/licenses/by/4.0/), which permits use, distribution and reproduction in any medium, provided the original work is properly cited.

Furman, 2014). Electrochemical polarization models for mineral sediments are based on surface complexation models that estimate the surface conductivity in the Stern and diffuse layers of the EDL (Leroy & Revil, 2009; Leroy et al., 2008; Revil & Skold, 2011). They yield a linear relationship between σ'' and the surface site density, Γ_s [sites m^{-2}], which can be determined from the cation exchange capacity (CEC) [$\text{mmol}_{\text{charge}} \text{g}_{\text{sed}}^{-1}$] and surface area, A_{surf} [$\text{m}^2 \text{g}_{\text{sed}}^{-1}$], using:

$$\Gamma_s = \frac{\text{CEC}}{A_{\text{surf}}} \quad (2)$$

so that the CEC, a comparatively easy to acquire bulk property of sediments, can reliably predict the polarizability of a sediment (Revil et al., 2023).

Here, we quantify the (linear) relationship between CEC and the σ'' of aquifer sediment cores, and over a broad range of OM-content in artificial mixtures of peat and calcite sand. We explore the applicability of EDL-based models for organic surfaces and derive petro-, or rather, *organo*-physical relationships between the total organic carbon (TOC) content and σ'' . We demonstrate that SIP can delineate zones rich in OM, and that even low fractions of OM (TOC <1%) significantly alter the electrical properties of unconsolidated media.

2. Materials and Methods

2.1. SIP Measurements on Field Cores

We extracted two fresh field cores (2.5–8.4 m depth, 51 mm diameter) from a 6–8 m thick confined Tufa aquifer characterized by autochthonous biogenic freshwater carbonates, near Tübingen, southwest Germany. The OM content of the sediments ranges from ~1% TOC to >50% TOC in naturally occurring peat layers. The cores were taken in the area investigated by Klingler et al. (2020) who delineated two extensive peat layers at depths of 4.0–4.2 and 5.55–5.9 m. Further information on the hydrogeological setting can be obtained from Martin et al. (2020). After extraction, the cores were sealed to prevent pore water leakage during transportation.

In the laboratory, we fitted 8 retracted electrodes with 15 cm spacing on the undisturbed 1.2 m liner sections. This allowed us to perform SIP measurements on the sediment without removing it from the liner, helping to maintain the same fully saturated water content as in the field. For this, a hollow 1.5 cm long cylinder (i.d. = 6 mm) was inserted into each hole drilled directly into the liner, and the inner cavity space was filled with agar (15 g L^{-1} in groundwater from the site). Copper electrodes ($d = 5$ mm) were inserted 5 mm into the liquid agar before gelification. We performed SIP measurements in a Wenner- α configuration (two current electrodes with two potential electrodes between them, all with equal spacing) with skip-0, leading to five measurements per core (see Figure S1 in Supporting Information S1 for a schematic illustration and a photograph of the set-up). Each measurement was assigned to the depth at the center between the potential electrodes. Phase shift ($-\varphi$) and impedance magnitude ($|Z|$) were measured at 12°C (corresponding to the site's groundwater temperature) over 45 log-frequency intervals between 0.1 and 1,000 Hz using a reference resistor of 100 Ω and an amplitude of 5 V (Portable SIP Unit, Ontash & Ermac Inc., USA). The results were converted to apparent frequency-dependent complex conductivities using a geometric factor, k [m], determined numerically for the current setup using pyGIMLi (Rücker et al., 2017). To compare the field-core measurements with the measurements on artificial peat-calcite mixtures, we performed a temperature correction of the conductivity magnitude $|\sigma|$ [S m^{-1}] following the procedure of Hayley et al. (2007):

$$|\sigma|^{20^\circ\text{C}} = |\sigma|^{12^\circ\text{C}} + 0.0183 \cdot (20.5^\circ\text{C} - 12^\circ\text{C}) \cdot |\sigma|^{12^\circ\text{C}} \quad (3)$$

We neglected the temperature effect on the φ spectra because the magnitude of φ has been shown to remain relatively constant with temperature, whereas the peak frequency drops with decreasing temperature (Bairlein et al., 2016). This simplification implies that the peak frequency measured in field cores is not directly comparable to that in the artificial peat-calcite mixtures. Following the SIP measurements, we used a splitter to open the cores and homogenized 15–25 cm long sections for TOC, water content/porosity, and CEC determination, following the procedures outlined in Text S1 of Supporting Information S1.

2.2. SIP Measurements of Artificial Peat-Calcite Mixtures

We prepared mixtures of peat, collected from the peat layer in the Tufa aquifer (study site), and calcite (marble) sand to mimic the composition of Tufa, while keeping the electrical conductivity (EC) during the SIP measurements constant. We used the same columns, tubing, pumps, and wet-packing procedure as Strobel, Abramov,

et al. (2023) and followed the approach of Mellage et al. (2022) of pore-volume replacement until the EC and pH of the in- and outflow were identical, to ensure chemical equilibrium prior to measurements. (Note: The columns were water saturated once packed and for the duration of the incubation). We used a CaCl₂ solution (EC = 1,100 μS cm⁻¹) as the saturating solution for the column experiments, mimicking the EC of the groundwater measured at wells in close proximity (<5 m) to the collected cores (aquifer EC = 1,100–1,300 μS cm⁻¹). The mineral phase of the Tufa is close to pure calcite (see Figure S2 in Supporting Information S1), however, the marble sand lacks the high intra-particle porosity of the Tufa (Strobel, Abramov, et al., 2023). Details on the sediment preparation and column packing, a photograph of the experimental set-up and schematic of the SIP measurements are shown in Text S2 and Figure S3 of Supporting Information S1.

Column SIP measurements were conducted as mentioned above, but with a higher spectral resolution (61 log-frequency intervals between 0.01 and 10,000 Hz) and at room temperature (20.5°C). The geometric factor of the columns was experimentally determined using measurements of the apparent EC of the columns filled with water of known conductivity. We packed triplicate columns for each SOM content (0%, 1%, 3%, 6%, 10%, 20%, 50% and 100% w/w). SIP measurements were performed at three locations using the upper, middle, and lower potential-electrode pairs (see Figure S3 in Supporting Information S1).

We also investigated the effect of porosity, associated with the volume changes caused by SOM addition, on the electrolytic conductivity σ_{el} [S m⁻¹], according to Archie's law (Archie, 1942). The real part of the complex conductivity was separated into an electrolytic contribution and a surface conduction contribution σ'_{surf} by (Vinegar & Waxman, 1984):

$$\sigma' = \sigma_{el} + \sigma'_{surf} = \sigma_{el} + \frac{\sigma''_{surf}}{l} \quad (4)$$

where $\sigma''_{surf} = \sigma''$ and $l = 0.042$, is a proportionality factor between the real and complex part of the surface conductivity as determined by Weller et al. (2013) for a frequency of 1 Hz. After the SIP measurements, the entire sediment of each column was removed and dried at 30°C for 3–7 d to determine the mass and, therefore, volume of water to compute the porosity, before proceeding with the quantification of the total TOC content and CEC (see Text S1 in Supporting Information S1 on details regarding the TOC and CEC quantification). The low temperature was chosen to avoid any compositional changes of the OM prior to CEC and TOC quantification (Enwezor, 1967).

3. Results and Discussion

3.1. Physical and Chemical Properties of the Field Cores

The TOC content, CEC, porosity, σ'' and σ' measured in the Tufa field cores are shown in Figure 1. Both Tufa field cores exhibit similar depth profiles of geochemical and geoelectrical properties. Three depth intervals (2.5–4.0 m, 4.2–5.6 m and 5.9–8.4 m) contain predominantly freshwater carbonates as the main solid component, whereas the two peat layers (4.0–4.2 m and 5.6–5.9 m) consist of 70%–90% OM and 10%–30% carbonates. In the upper Tufa section, where OM was present as mm to cm thick layers, the TOC content was lowest with a minimum of 2.3%. Below the main peat layer at 5.8 m, the Tufa exhibits alternating carbonate deposits and small, often discontinuous mm-thick peat layers between the two cores, yielding a very high cm-scale variability in TOC from less than 5% up to 22%. In the peat layers, the TOC content reaches up to 56%. The variability in the chemical composition with depth is also reflected in the CEC (Figure 1b), as a metric for changing surface charge, and the porosity (Figure 1c), as a proxy for changes in the pore structure and pore network. Both CEC and porosity increase with increasing TOC content. However, the increase in CEC is more pronounced, with an up to 10-fold increase in CEC from the low TOC regions to the peat layers, whereas the porosity increases from a minimum of 68% to up to 83% in the peat.

The complex conductivity measurements also reveal a strong variability of both σ'' (Figure 1d) and σ' (Figure 1e) as a function of depth. In depth intervals with low TOC, σ'' and σ' are also lower, with values of approximately 1.3–2.7 and 400–490 μS cm⁻¹, respectively, and high in the peat layers, reaching up to 3.7–5.5 and 470–590 μS cm⁻¹, respectively. While both show an increasing trend with increasing TOC content, we observe a 4.2-fold increase of the imaginary part but only a 1.5-fold increase in the real part, highlighting that there are substantial changes in the electrical properties of the sediment surface associated with TOC rather than electrolytic conduction.

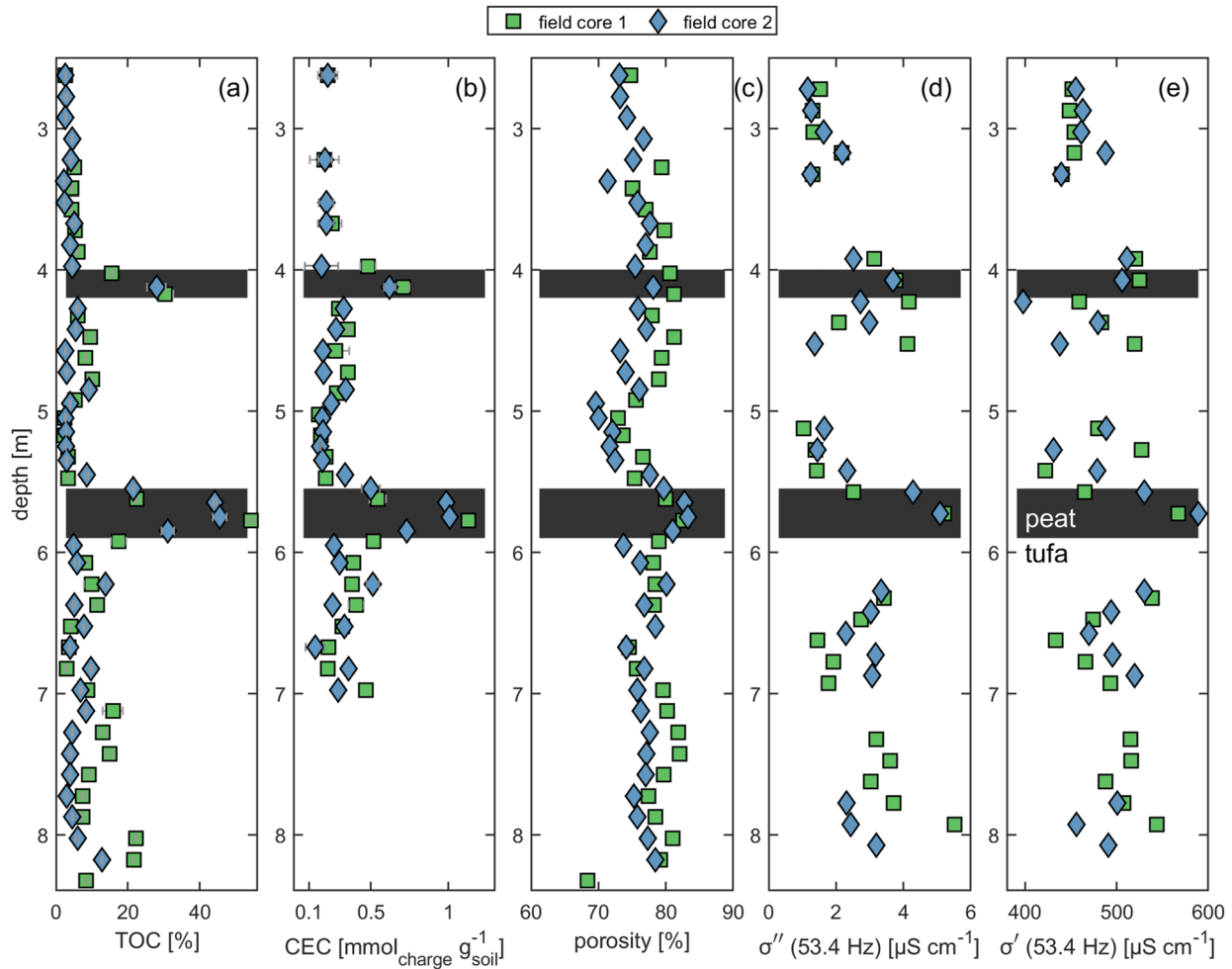


Figure 1. Overview of the field core data, showing the (a) total organic carbon (TOC), (b) cation exchange capacity (CEC), (c) porosity, as well as the (d) imaginary and (e) real part of the complex conductivity at 53.4 Hz depth resolved from 2.5 to 8.4 m depth. Error bars in the TOC and CEC subplots indicate the standard deviation of triplicate measurements and the background colors indicate the sediment characterization as either tufa (white) or peat (dark gray).

The field cores show evidence of a correlation between the TOC content and the imaginary conductivity of the sediment ($R^2 = 0.67$). We believe that the weak correlation is due to the experimental design and the inherent complexity of field samples, yielding a larger spread in the data. Measurement errors resulting from the installation of the electrodes at the core liners (current injection was performed at retracted electrodes) and from partial desaturation of the sediment during the drilling and transport of the cores to the laboratory likely contributed to this spread. Furthermore, we assigned the depth of the SIP measurements to the midpoint of the electrode array. However, SIP signals are sensitive to a volume interval rather than a single point (Mellage et al., 2018). The heterogeneity of the sediment (see Figure S4 in Supporting Information S1 for core photographs), stemming from an irregular sequence of speckled carbonates and peat, likely also led to a slight discrepancy between the SIP measurements and the volume-averaged TOC and CEC. Finally, the, potentially depth-dependent chemistry and EC of the pore water was neither monitored nor held constant for the field cores. (Note: No pore water samples were extracted from the cores to avoid water loss and allow an accurate estimation of porosity). Therefore, we further investigated the relationship between TOC content and complex conductivity using artificial peat-calcite mixtures under more controlled conditions with constant pore water chemistry and conductivity.

3.2. Complex Conductivity of Artificial Peat-Calcite Mixtures and Field Cores

The relationships between complex conductivity (50 Hz) and TOC, CEC, and porosity in the artificial peat-sand mixtures are shown in Figure 2, together with the linear regressions of the real and imaginary conductivities

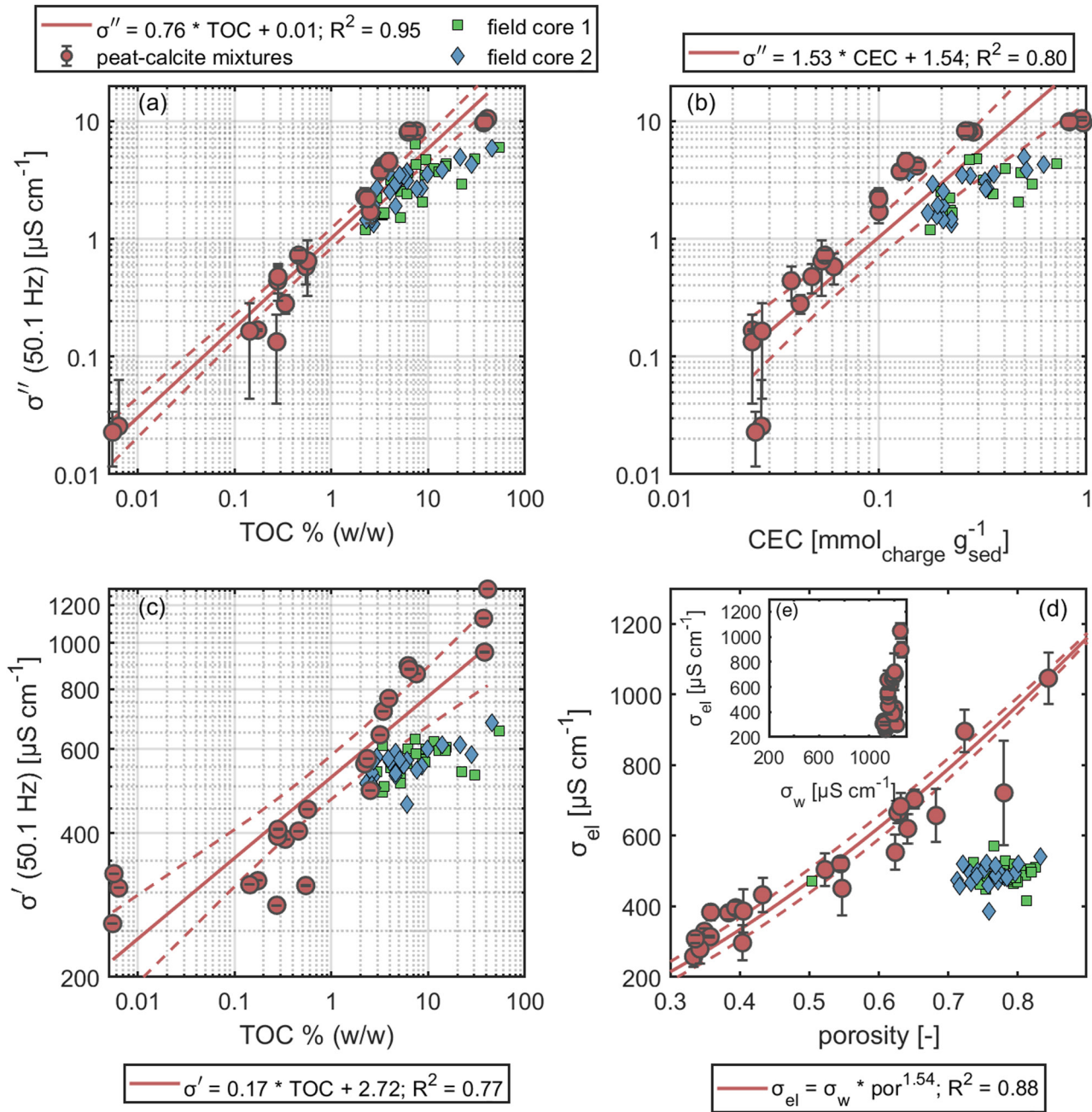


Figure 2. Regressions of the complex electrical conductivity. (a): σ'' versus total organic carbon (TOC) content, (b) σ'' versus cation exchange capacity, (c) σ' versus TOC, (d) electrolytic conductivity versus porosity, (e) electrolytic conductivity versus pore water conductivity. Red markers: artificial peat-calcite mixtures; blue/green markers: measurements on field cores from the Tufa aquifer. Error bars of the peat-calcite mixtures show the standard deviation between the three measurements in one column.

with TOC and CEC (Figures 2a–2c) and Archie's law for the electrolytic conductivity as a function of porosity (Figure 2d). Both σ'' and σ' are presented as average values of all three potential electrode pairs in each triplicate to reduce the variability associated with the packing procedure. The eight different peat-calcite mixtures enabled us to cover a broad range of TOC values spanning over four orders of magnitudes from a trace amount of less than 0.01% in the pure calcite columns to 41% TOC in the pure peat columns. In Figure 2a, we show the relationship between the mean σ'' at 50 Hz and the TOC content of each column. We chose 50 Hz because this is the approximate peak frequency of the peat spectra (spectral data are discussed below), the dominant solid fraction that contributes to polarization. (Note: The relationships in Figure 2 are consistent across the measured

frequency range—data not shown). Figure 2a shows a strong positive correlation between σ'' and TOC content. The pore-water composition (i.e., EC) was held constant in the experiment. Therefore, the σ'' -TOC relationship, with a 525-fold increase from $0.02 \mu\text{S cm}^{-1}$ in calcite sand up to $10.5 \mu\text{S cm}^{-1}$ in pure peat, highlights the strong control of OM-polarization, that is, charge storage, on the magnitude of σ'' . While σ' is also positively correlated with the TOC content of the peat-calcite mixtures (red markers in Figure 2c), its much lower relative increase compared to σ'' of a factor 4.4 indicates more substantial changes in the charge-storage properties than in electrolytic and surface conduction of the column fillings with high OM content.

The SIP measurements on the field cores, plotted onto the lab-derived relationships, align very well with the artificial peat-calcite mixtures (green and blue markers in Figure 2), in particular for σ'' and TOC contents between 1% and 10%. At higher TOC contents, the σ'' of the field cores is considerably lower than that of the peat-calcite mixtures. Moreover, the similar magnitude in σ' between the peat-sand mixtures and field cores (Figure 2c) highlights that allowing the 5 mM CaCl_2 packing solution to equilibrate with the peat-sand pack was successful at mimicking the pore-water composition of the Tufa in the laboratory. However, the relationship between the TOC content and σ' seems to follow a different trend in the field cores than in the peat-sand columns, exhibiting a more gradual slope in the field cores. As discussed in Section 3.1, the more controlled laboratory experiment addressed some of the sources of error associated with our measurements on field cores, which we believe are the cause of the differences in slope between peat-sand mixtures and field samples. Moreover, the unknown depth variability in the pore water chemistry of the field cores likely also contributed to the slight offset in σ'' in the field cores compared to the artificial mixtures. We speculate that the OM-calcite association in the Tufa may also be a contributing factor. Peat and calcite sand were only mixed macroscopically in the artificial mixtures but remain separate at the microscopic-level. Conversely, in the aquifer setting of the field cores, OM co-sedimented with the Tufa particles, potentially even stabilizing and binding the calcite nano-crystals (Strobel, Abramov, et al., 2023) that make up the Tufa aggregates. Thus, part of the OM surface in the undisturbed field cores may be “blocked” for polarization, as was already hypothesized by Mellage et al. (2022) and Schwartz and Furman (2014) in the context of organo-mineral complexes.

To gain further insights into the relevant properties of OM that determine its polarization potential, we considered changes in the surface properties (i.e., CEC) and pore structure (i.e., porosity). The addition of OM yielded both an increase in CEC and porosity with increasing TOC content (Figure S5 in Supporting Information S1). Consequently, σ'' is also positively correlated with CEC and porosity (Figure 2b and Figure S5c in Supporting Information S1). The influence of the CEC and a linear relationship between σ'' and CEC is in agreement with existing grain-based polarization models for mineral surfaces and bacteria (e.g., Leroy et al., 2008; Revil et al., 2012).

Interpreting the dependence of the complex EC on changes in the pore structure or porosity is more difficult than that on CEC. Existing models and the joint interpretation of the artificial mixtures and field cores point toward a limited effect of the porosity on σ'' . Porosity affects electrolytic conduction, as described by Archie's law (Archie, 1942). We observed variations in porosity related to OM content. To separate the electrolytic and surface conduction contributions to σ' and to separate the effect of porosity and surface polarization on σ' , we applied Equation 4. We acknowledge that our approach is only an approximation because the frequency-dependence of the proportionality factor l has not been investigated or estimated yet and might be different at 50 Hz compared to 1 Hz (i.e., the frequency it was derived for). Nevertheless, because the resulting electrolytic conductivity follows Archie's law (Text S3 in Supporting Information S1), with a cementation exponent of 1.54 (Figure 2d), in agreement with cementation exponents for unconsolidated sands (Friedman, 2005), we believe that Equation 4 provides a good first-order approximation of the relative contribution of σ_{el}' and σ_{surf}' to σ' . Based on this analysis, only about one fifth of the total increase in σ' from calcite sand to pure peat can be attributed to an increase in σ_{surf}' . Moreover, the field-core measurements (blue and green markers in Figure 2d) show a much lower variability in the porosity and almost constant electrolytic conductivity for all measurements, which points toward a significant contribution to the high porosity of the calcite aggregates that make up the Tufa in the field. The marble sand grains in the artificial calcite-peat mixtures lack the secondary porosity of the carbonaceous Tufa thus yielding the wider spread in porosity in our artificial mixtures. This discrepancy may also contribute to the difference in slope of σ' of the field cores and the artificial mixtures (Figure 2c). Nonetheless, the lack of pore-structural changes (or less significant ones) in the field cores coupled to the TOC- σ'' and CEC- σ'' relationships provides strong evidence that porosity plays a minor role in controlling the changes in polarization.

While we cannot fully disentangle the relative effects of pore-structure changes and an increase in surface-site density, existing theory and the excellent agreement between the artificial peat-calcite mixtures and field cores for the relationship between σ'' and CEC (Figure 2b) strongly suggest that our results are driven by polarization

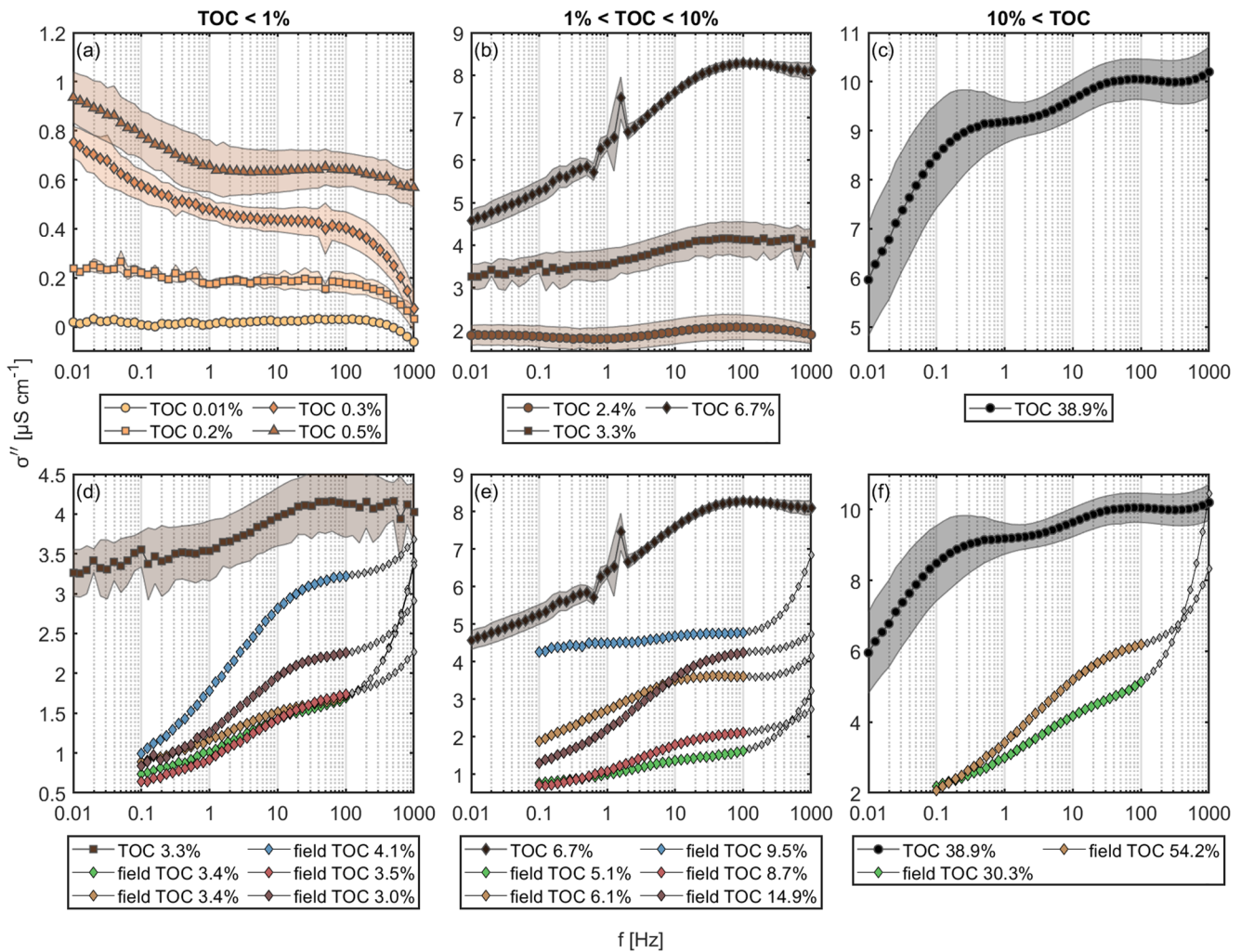


Figure 3. Imaginary conductivity (σ'') spectra of the peat-calcite mixtures. (a): low, (b): medium, (c): high total organic carbon (TOC) contents. The spectra are the averages of triplicates for each treatment, showing their mean value and the standard deviation as a shaded area. In panels (d–f), the spectra of the artificial peat-calcite mixtures are compared to spectra of field core sections with comparable TOC contents. Markers above 100 Hz for field measurements are colored in gray, denoting the lack of confidence in these data related to measurement biases inherent to the electrode array used on the field cores. (Note: the different y-axis scaling for each panel.)

stemming from the OM surfaces. Furthermore, the linear relationship between the CEC and σ'' suggests that polarization in our OM-containing sediments is driven by processes analogous to those at mineral surfaces.

4. The Polarization of Organic Matter: σ'' Spectra

In Figures 3a–3c we show the σ'' -spectra separately for low, medium, and high TOC contents (see Figure S6 in Supporting Information S1 for an overview of all σ'' spectra). Apart from a general increase of σ'' at all frequencies, we observe a shift in peak frequency from less than 0.01 Hz for TOC < 1% to 50 Hz in the medium- and high-TOC content mixtures. In addition, the pure peat exhibited a secondary polarization with a peak frequency at about 1.5 Hz. The frequency peak is related to the timescale of polarization. Higher frequencies suggest shorter timescales for relaxation and back-diffusion. The time scale is controlled by the chemical properties of the EDL and the length-scale over which ion migration occurs. Thus, for a system with similar chemical properties, changes in peak frequency suggest a shift in the dominant polarization length scale (e.g., Schwarz (1962), for spherical grains). Assuming that the polarization response is entirely related to the OM and applying the relationship between relaxation time and the polarization length scale (Weller & Slater, 2019) with a constant surface-diffusion coefficient, the shift in peak frequency would correspond to a decrease of the dominant polarization length scale by a factor of about 100. We attribute this shift toward lower polarization length scales to a

transition from polarization over single, isolated OM particles in a calcite-sand matrix to the formation of a pore structure network of connected OM particles in which the pore size is now the dominant polarization length scale. In that context, the polarization of pure peat (Figure 3c) would indicate the presence of two main pore sizes. This aligns well with the fact that peat is known to have two dominant pore sizes (dual-porosity) that control the flow of water (Kleimeier et al., 2017; Rezanezhad et al., 2012, 2016), which likely also influence current flow and polarization.

Figures 3d–3f compare the spectra of field cores with those of the artificial mixtures for similar TOC contents. Due to the linear scale of the y-axis, the lower σ'' response in the field cores becomes more prevalent than in Figure 2, but the spectral characteristics are still comparable. (Note: The differences in magnitude between field-core spectra and spectra from the artificial mixtures relate to the differences discussed in Section 3.2, pertaining to the single-frequency relationships that were derived from the spectral responses). Both, field cores and artificial mixtures show an increase in σ'' with increasing frequency and a peak frequency at about 50 Hz. This also holds for the measurements in pure peat, where the field-core spectra lack the secondary peak at about 1.5 Hz (Figure 3f) indicating that it might be an artifact of the repacking of the peat into columns.

5. Conclusions

Solid OM can change the σ'' response of a sediment by several orders of magnitude and should therefore not be neglected in the interpretation of complex conductivity data. Therefore, to prevent data-misinterpretation, the quantification of TOC should be an integral part of the sediment characterization for ground-truthing of (S)IP surveys, in particular, when interpreting data in soils or other OM rich porous media. Our results suggest that the high CEC is the main property of OM that determines its polarization strength.

With a CEC of $1.3 \text{ mmol}_{\text{charge}} \text{ g}_{\text{sed}}^{-1}$, the OM used in this study is comparable to 2:1 clay minerals of very high CEC (e.g., vermiculite with reported CEC values of 1–1.5 $\text{mmol}_{\text{charge}} \text{ g}_{\text{sed}}^{-1}$) and considerably higher than 1:1 clay minerals such as kaolinite (0.03–1.5 $\text{mmol}_{\text{charge}} \text{ g}_{\text{sed}}^{-1}$) or illite (0.1–0.4 $\text{mmol}_{\text{charge}} \text{ g}_{\text{sed}}^{-1}$) (Carrol, 1959). Given that the chemical composition of OM is site specific and depends on many factors (e.g., origin of OM, degree of decomposition, pH), the relationship between σ'' and TOC content derived in this work is also specific for the type of OM (peat) used here and should not be directly applied to other systems. A difference in the OM composition and thus also CEC may explain the contrasting results reported by the handful of previous studies that investigated the effect of OM on SIP signals versus this work. Future work on different OM types and mixtures with other polarizing sediment components such as clay minerals could shed light on their relative importance under different environmental conditions. Furthermore, the complex conductivity signal of pure peats will require further investigation to better understand what mechanisms determine the σ'' -signal in peatlands. Given that the CEC of OM is expected to highly depend on pH (Helling et al., 1964), an in-depth characterization of the geochemical conditions in peatlands will be necessary to understand the variability of the complex conductivity signal in purely organic environments.

In addition to highlighting the importance of considering OM in SIP signal interpretation, the findings herein, highlight the relevance of geophysical methods for the characterization of OM-rich soils and peatlands. Such applications are poised to improve our capabilities to monitor carbon cycling at higher spatial and temporal scales in vulnerable, and rapidly changing environments in the era of climate change.

Data Availability Statement

The SIP data, the geochemical data and the data processing and analysis scripts are available at Strobel, Doerrich, et al. (2023).

References

- Archie, G. E. (1942). The electrical resistivity log as an aid in determining some reservoir characteristics. *Transactions of the AIME*, 146(01), 54–62. <https://doi.org/10.2118/942054-g>
- Bairlein, K., Bucker, M., Hördt, A., & Hinze, B. (2016). Temperature dependence of spectral induced polarization data: Experimental results and membrane polarization theory. *Geophysical Journal International*, 205(1), 440–453. <https://doi.org/10.1093/gji/ggw027>
- Binley, A., & Slater, L. (2020). *Resistivity and induced polarization: Theory and applications to the near-surface earth*. Cambridge University Press.

Acknowledgments

Adrian Mellaage would like to acknowledge the financial support of the Baden-Württemberg Stiftung received for this project via the Eliteprogramme for Postdocs. The authors gratefully acknowledge Bernice Nisch, Carsten Leven and Christoph Berthold for their support with TOC measurements, field work and pXRD measurements and Thomas Günther for his support with pyGIMLI. Open Access funding enabled and organized by Projekt DEAL.

- Bücker, M., Flores Orozco, A., Undorf, S., & Kemna, A. (2019). On the role of stern- and diffuse-layer polarization mechanisms in porous media. *Journal of Geophysical Research: Solid Earth*, *124*(6), 5656–5677. <https://doi.org/10.1029/2019JB017679>
- Carrol, D. (1959). Ion exchange in clays and other minerals. *Geological Society of America Bulletin*, *70*(6), 749. [https://doi.org/10.1130/0016-7606\(1959\)70\[749:IEICAO\]2.0.CO;2](https://doi.org/10.1130/0016-7606(1959)70[749:IEICAO]2.0.CO;2)
- Enwezor, W. O. (1967). Soil drying and organic matter decomposition. *Plant and Soil*, *26*(2), 269–276. <https://doi.org/10.1007/bf01880177>
- Flores Orozco, A., Gallistl, J., Steiner, M., Brandstätter, C., & Fellner, J. (2020). Mapping biogeochemically active zones in landfills with induced polarization imaging: The Heferlbach landfill. *Waste Management*, *107*, 121–132. <https://doi.org/10.1016/j.wasman.2020.04.001>
- Friedman, S. P. (2005). Soil properties influencing apparent electrical conductivity: A review. *Computers and Electronics in Agriculture*, *46*(1–3), 45–70. <https://doi.org/10.1016/j.compag.2004.11.001>
- Hayley, K., Bentley, L. R., Gharibi, M., & Nightingale, M. (2007). Low temperature dependence of electrical resistivity: Implications for near surface geophysical monitoring. *Geophysical Research Letters*, *34*(18), L18402. <https://doi.org/10.1029/2007GL031124>
- Helling, C. S., Chesters, G., & Corey, R. B. (1964). Contribution of organic matter and clay to soil cation-exchange capacity as affected by the pH of the saturating solution. *Soil Science Society of America Journal*, *28*(4), 517–520. <https://doi.org/10.2136/sssaj1964.03615995002800040020x>
- Katona, T., Gilfedder, B. S., Frei, S., Bücker, M., & Flores Orozco, A. (2021). High-resolution induced polarization imaging of biogeochemical carbon-turnover hot spots in a peatland. *Biogeosciences*, *18*(13), 4039–4058. <https://doi.org/10.5194/bg-18-4039-2021>
- Kleimeier, C., Rezaeezhad, F., van Cappellen, P., & Lennartz, B. (2017). Influence of pore structure on solute transport in degraded and undegraded fen peat soils. *Mires Peat*, *19*(18), 1–9.
- Klingler, S., Cirpka, O. A., Werban, U., Leven, C., & Dietrich, P. (2020). Direct-Push color logging images spatial heterogeneity of organic carbon in floodplain sediments. *Journal of Geophysical Research: Biogeosciences*, *125*(12), e2020JG005887. <https://doi.org/10.1029/2020JG005887>
- Leroy, P., & Revil, A. (2009). A mechanistic model for the spectral induced polarization of clay materials. *Journal of Geophysical Research*, *114*(B10), B10202. <https://doi.org/10.1029/2008JB006114>
- Leroy, P., Revil, A., Kemna, A., Cosenza, P., & Ghorbani, A. (2008). Complex conductivity of water-saturated packs of glass beads. *Journal of Colloid and Interface Science*, *321*(1), 103–117. <https://doi.org/10.1016/j.jcis.2007.12.031>
- Martin, S., Klingler, S., Dietrich, P., Leven, C., & Cirpka, O. A. (2020). Structural controls on the hydrogeological functioning of a floodplain. *Hydrogeology Journal*, *28*(8), 2675–2696. <https://doi.org/10.1007/s10040-020-02225-8>
- Mellage, A., Holmes, A. B., Linley, S., Vallée, L., Rezaeezhad, F., Thomson, N. R., et al. (2018). Sensing coated iron-oxide nanoparticles with spectral induced polarization (SIP): Experiments in natural sand packed flow-through columns. *Environmental Science & Technology*, *52*(24), 14256–14265. <https://doi.org/10.1021/acs.est.8b03686>
- Mellage, A., Zakai, G., Efrati, B., Pagel, H., & Schwartz, N. (2022). Paraquat sorption- and organic matter-induced modifications of soil spectral induced polarization (SIP) signals. *Geophysical Journal International*, *229*(2), 1422–1433. <https://doi.org/10.1093/gji/ggab531>
- Ponziani, M., Slob, E. C., Vanhala, H., & Ngan-Tillard, D. (2012). Influence of physical and chemical properties on the low-frequency complex conductivity of peat. *Near Surface Geophysics*, *10*(6), 491–501. <https://doi.org/10.3997/1873-0604.20111037>
- Revil, A., Atekwana, E. A., Zhang, C., Jardani, A., & Smith, S. (2012). A new model for the spectral induced polarization signature of bacterial growth in porous media. *Water Resources Research*, *48*(9). <https://doi.org/10.1029/2012WR011965>
- Revil, A., Ghorbani, A., Jougnot, D., & Yven, B. (2023). Induced polarization of clay-rich materials—Part I: The effect of desiccation. *Geophysics*, *88*(4), 1–57. <https://doi.org/10.1190/geo2022-0510.1>
- Revil, A., & Skold, M. (2011). Salinity dependence of spectral induced polarization in sands and sandstones. *Geophysical Journal International*, *187*(2), 813–824. <https://doi.org/10.1111/j.1365-246X.2011.05181.x>
- Rezaeezhad, F., Price, J. S., & Craig, J. R. (2012). The effects of dual porosity on transport and retardation in peat: A laboratory experiment. *Canadian Journal of Soil Science*, *92*(5), 723–732. <https://doi.org/10.4141/CJSS2011-050>
- Rezaeezhad, F., Price, J. S., Quinton, W. L., Lennartz, B., Milojevic, T., & Van Cappellen, P. (2016). Structure of peat soils and implications for water storage, flow and solute transport: A review update for geochemists. *Chemical Geology*, *429*, 75–84. <https://doi.org/10.1016/j.chemgeo.2016.03.010>
- Rücker, C., Günther, T., & Wagner, F. M. (2017). pyGIMLi: An open-source library for modelling and inversion in geophysics. *Computers & Geosciences*, *109*, 106–123. <https://doi.org/10.1016/j.cageo.2017.07.011>
- Schwartz, N., & Furman, A. (2014). On the spectral induced polarization signature of soil organic matter. *Geophysical Journal International*, *200*(1), 589–595. <https://doi.org/10.1093/gji/ggu410>
- Schwarz, G. (1962). A theory of the low-frequency dielectric dispersion of colloidal particles in electrolyte solution. *The Journal of Physical Chemistry*, *66*(12), 2636–2642. <https://doi.org/10.1021/j100818a067>
- Slater, L. D., & Glaser, D. R. (2003). Controls on induced polarization in sandy unconsolidated sediments and application to aquifer characterization. *Geophysics*, *68*(5), 1547–1558. <https://doi.org/10.1190/1.1620628>
- Strobel, C., Abramov, S., Huisman, J. A., Cirpka, O. A., & Mellage, A. (2023). Spectral induced polarization (SIP) of denitrification-driven microbial activity in column experiments packed with calcareous aquifer sediments. *Journal of Geophysical Research: Biogeosciences*, *128*(1), e2022JG007190. <https://doi.org/10.1029/2022JG007190>
- Strobel, C., Doerrich, M., Stieff, E.-H., Huisman, J. A., Cirpka, O. A., & Mellage, A. (2023). Electronic appendix to: Organic matter matters—The imaginary conductivity of sediments rich in solid organic carbon [Dataset]. Zenodo. <https://zenodo.org/records/8362608>
- Vinegar, H. J., & Waxman, M. H. (1984). Induced polarization of shaly sands. *Geophysics*, *49*(8), 1267–1287. <https://doi.org/10.1190/1.1441755>
- Weller, A., Slater, L., & Nordsiek, S. (2013). On the relationship between induced polarization and surface conductivity: Implications for petrophysical interpretation of electrical measurements. *Geophysics*, *78*(5), D315–D325. <https://doi.org/10.1190/geo2013-0076.1>
- Weller, A., & Slater, L. D. (2019). Permeability estimation from induced polarization: An evaluation of geophysical length scales using an effective hydraulic radius concept. *Near Surface Geophysics*, *17*(6), 581–594. <https://doi.org/10.1002/nsg.12071>

References From the Supporting Information

- Rühlmann, J., Körschens, M., & Graefe, J. (2006). A new approach to calculate the particle density of soils considering properties of the soil organic matter and the mineral matrix. *Geoderma*, *130*(3), 272–283. <https://doi.org/10.1016/j.geoderma.2005.01.024>
- Sumner, M. E., & Miller, W. P. (1996). Cation exchange capacity and exchange coefficients. In D. L. Sparks, A. L. Page, P. A. Helmke, R. H. Loeppert, P. N. Soltanpour, M. A. Tabatabai, et al. (Eds.), *Methods of soil analysis* (pp. 1201–1229). Soil Science Society of America, American Society of Agronomy (SSSA Book Series).